Chemical Engineering Science 195 (2019) 820–827

Contents lists available at ScienceDirect

Chemical Engineering Science

journal homepage: www.elsevier.com/locate/ces

Direct simulations of two-phase flow experiments of different geometry complexities using Volume-of-Fluid (VOF) method

X. Yin [a,*,1], I. Zarikos [a], N.K. Karadimitriou [b], A. Raoof [a], S.M. Hassanizadeh [a]

[a] Department of Earth Sciences, Utrecht University, Utrecht, the Netherlands
[b] Institute of Mechanics (CE), University of Stuttgart, Stuttgart, Germany

HIGHLIGHTS

- Two-phase flow in porous media of different geometry complexities are simulated using Volume-of-Fluid (VOF) method.
- Flow patterns and their temporal evolutions are compared between simulations and experiments.
- VOF method reproduced well capillary rise experiment.
- Possible reasons for discrepancy between simulation and experiment with more complex geometries are analyzed.

ARTICLE INFO

Article history:
Received 6 July 2018
Received in revised form 21 September 2018
Accepted 21 October 2018
Available online 23 October 2018

Keywords:
Volume of Fluid (VOF) method
Two-phase flow
Porous media
Pore-scale simulations

ABSTRACT

Two-phase flow in three porous media with different geometry complexities are simulated using the Volume-of-Fluid (VOF) method. The evolution of the flow pattern, as well as the dynamics involved are simulated and compared to experiments. For a simple geometry and smooth solid surface, like single capillary rise experiment, VOF simulation gives results which are in good agreement with the experiments. For a micromodel, with a relatively simple geometry, we can predict the flow pattern while we cannot effectively capture the dynamics of the process in terms of the temporal evolution of flow. With an increase in the geometry complexity in another micromodel, we fail to predict both the flow pattern and the flow dynamics. The reasons for this failure are discussed: interface modeling, pinning of contact line, 3D effects and the sensitivity of the system to initial and boundary conditions. More work regarding benchmarking of pore-scale methods in combination with experiments with different geometry complexities is needed. Also, possibilities and the potential to make better use of the porous media structure data from advanced visualization methods should be addressed.

1. Introduction

Many environmental, industrial and agricultural applications share the same underlying physics of immiscible multiphase flow in porous media. Complex geometry and flow events happening on different spatial and temporal scales make it more difficult to model and simulate than its single phase counterpart (Wooding and Morel-Seytoux, 1976), on both continuum and pore-scale. Continuum-scale modeling usually does not consider the pore structure explicitly (Richards, 1931; Van Genuchten, 1980), and only average quantities over a representative elementary volume (REV) are considered. On the contrary, pore-scale simulations can give the local velocities and pressures of interest, and provide constitutive relationships for continuum-scale models.

With the development of various visualization techniques (Kaestner et al., 2008; Bultreys et al., 2016), the pore structure can be obtained at a quite high spatial resolution, and pore-scale models can thus better simulate the system utilizing these information. As a computationally efficient method, pore-network model (PNM) has evolved over the last decades (Blunt, 2001) and quasi-static PNM has been successfully employed for the prediction of the relative permeability and capillary pressure-saturation relation in multiphase flow system (Oren et al., 1998). When viscous forces need to be considered, dynamic PNM should be employed. However, simplified porous structures and physics are usually assumed in dynamic PNM. Numerical simulation methods, like Lattice Boltzmann method (LBM) (Kang et al., 2002), Smoothed Particle Hydrodynamic (SPH) method (Hirschler et al., 2016) and

* Corresponding author.
E-mail addresses: xiaoguang.yin@sz.tsinghua.edu.cn (X. Yin), s.m.hassanizadeh@uu.nl (S.M. Hassanizadeh).
[1] Present address: Engineering Laboratory for Functionalized Carbon Materials, Graduate School at Shenzhen, Tsinghua University, China.

https://doi.org/10.1016/j.ces.2018.10.029
0009-2509/

Computational Fluid Dynamics (CFD) approaches (Raeini et al., 2012) can resolve the high spatial resolution geometry. In many works numerical accuracy and/or stability of these methods are examined, but usually very simple scenarios are considered: like a droplet resting on a flat/cylindrical surface, free rising bubbles in quiescent liquids, and moving droplets in uniform velocity field. For porous media with a complex geometry, different pore-scale methods have been employed to simulate the two-phase flow in 2D micromodels, where better control, observation and measurement of the system can be achieved.

Horgue et al. (2013) used micromodels to study spreading of a liquid jet in periodic array of cylinders and they observed flow rate dependent flow regimes. Their VOF simulation obtained flow regimes which are similar to those observed in the experiments. The main difference between simulation and experiment concerned the precise values of the threshold flow rate for regime transitions from one to another. They proposed that the effects related to dynamic films and complex menisci are responsible for the discrepancy.

Ferrari et al. (2015) presented a comparison of VOF simulations and experiments for unstable primary drainage in porous micromodels. Same flux boundary conditions were used in the simulation as in the experiment. Different percolation patterns from experiment and numerical simulation was reported. Three main sources of error were identified for the mismatch between the models and the experiments: the uncertainty on the pore space geometry used so as to simulate the experiment, the inaccuracy in initial condition and three-dimensional effects.

Kunz et al. (2015) developed an improved SPH model that can track the moving interfaces during two-phase flow and account for wall-fluid-fluid interactions. The numerical model was applied to the simulation of a dynamic micromodel experiment. The simulated flow pattern was found to be in good agreement with the experiment, while the dynamics of the experiment was not well reproduced in terms of temporal synchronization of the model with the experiment.

Ling et al. (2017) investigated the reproductivity of pore-scale multiphase flow experiments in replicates of the micromodel under small capillary number. Six replicates were manufactured and up to five experiments were conducted in each replica. Smaller variability in flow patterns was observed in drainage experiments. They then used STAR-CCM+ (using finite volume discretization and VOF method for interface tracking) to simulate the experiment deterministically and stochastically by imposing same flow rate as in experiment or randomly varying flow rate. In this way they demonstrated that variations in the flow pattern were due to sub-porescale geometry differences in micromodels and variations in the boundary conditions.

Xu et al. (2017) proposed a new algorithm for imposing a contact angle in LBM. Furthermore, simulations of drainage and imbibition experiments in a micromodel were conducted. The same viscosity ratio was used in the simulations as in the experiments while capillary number employed in the simulations was 4 orders of magnitude higher than the experimental value. They found quantitatively good agreement in flow patterns between simulation and experiment.

All the simulations, except the work by Kunz et al. (2015), used flux boundary conditions as those in experiments, and compared the resulting flow patterns with experiments. Pressure gradient boundary conditions were applied in the simulation as in experiments in Kunz et al. (2015). Also, usually only one micromodel geometry was reported simulated by the pore-scale methods.

In this work, we present pore-scale simulations of multiphase flow in geometries of different complexities using VOF method in OpenFOAM (Weller et al., 1998). Both flow pattern and flow rate-pressure correspondence between experiment and numerical simulation are addressed.

2. Numerical model description

2.1. Description of VOF method

For single phase flow the Navier-Stokes equations for mass and momentum balance (assume incompressibility and ignore external body forces) are used:

$$\nabla \cdot \mathbf{u} = 0 \tag{1}$$

$$\frac{\partial \rho \mathbf{u}}{\partial t} + \nabla \cdot (\rho \mathbf{u}\mathbf{u}) = -\nabla p + \nabla \cdot (2\mu \mathbf{E}) \tag{2}$$

where $\mathbf{u}$ is velocity, ρ is density, μ is viscosity, $\mathbf{E}$ is the deformation rate tensor, and p is pressure.

For the direct simulation of two-phase flow, we can solve Navier-Stokes equations for each phase and impose appropriate boundary conditions at the sharp fluid-fluid interface. But this generally requires interface fitting grids, which is impractical for cases involving interface merging or collapsing. An alternative approach, the VOF method, has been introduced as a diffuse interface model, in the sense that sharp interface is smoothed over layers of finite thickness. In this method, the computational domain is divided into 3 regions: two regions each for a single phase and a transition layer region for the interface. A volume fraction function, α, is used to delineate the three regions:

$$\alpha = \begin{cases} 1 & \text{in the wetting phase} \\ 0 & \text{in the non-wetting phase} \\ (0,1) & \text{in the interface region} \end{cases} \tag{3}$$

The interfacial force $\mathbf{f}_s$ is responsible for capillary pressure induced at the interface, and is modeled as a volumetric force, for a smooth transition region with a continuous α (Brackbill et al., 1992):

$$\mathbf{f}_s \approx \mathbf{f}_v = \sigma k \nabla \alpha \tag{4}$$

where σ is the interfacial tension between the wetting phase and the non-wetting phase, and k is the curvature of interface defined as:

$$k = -\nabla \cdot \mathbf{n} = -\nabla \cdot \left(\frac{\nabla \alpha}{\|\nabla \alpha\|}\right) \tag{5}$$

with $\mathbf{n}$ standing for the local normal unit vector.

In order to be consistent with the mass and momentum balance equations for each single phase, density and viscosity are volume fraction functions weighted:

$$\rho = \alpha \rho_w + (1-\alpha)\rho_{nw} \tag{6}$$

$$\mu = \alpha \mu_w + (1-\alpha)\mu_{nw} \tag{7}$$

Momentum balance equation evolves into:

$$\frac{\partial \rho \mathbf{u}}{\partial t} + \nabla \cdot (\rho \mathbf{u}\mathbf{u}) = -\nabla p + \nabla \cdot (2\mu \mathbf{E}) + \mathbf{f}_v \tag{8}$$

In each single phase region, the Navier-Stokes equation still applies for that phase; while at interface domain where $0 < \alpha < 1$, extra volumetric force $\mathbf{f}_v$ takes into account the capillary pressure drop across the interface. In OpenFOAM, to maintain the sharpness of the interface region, an artificial compression term is added to the transport equation of α:

$$\frac{\partial \alpha}{\partial t} + \nabla \cdot (\alpha \mathbf{u}) + \nabla \cdot (\alpha(1-\alpha)\mathbf{u}_r) = 0 \tag{9}$$

where compression velocity $\mathbf{u}_r$ is formulated based on maximum velocity magnitude in the interface domain.

The contact angle, θ, is included by condition at contact line:

$$\mathbf{n}_{\delta_s} = \mathbf{n}_s \cos\theta + \mathbf{t}_s \sin\theta \tag{10}$$

where $\mathbf{n}_s$ is the unit vector normal to the solid wall, $\mathbf{n}_{\delta_s}$ is the unit vector normal to the interface and $\mathbf{t}_s$ is the unit vector perpendicular to the contact line, tangent to and pointing into wetting-solid interface surface.

2.2. Corrected-two-dimensional model

Micromodel experiments are three-dimensional in nature, considering the relatively small and uniform depth, it is computationally efficient to solve the problem in two-dimension by taking into account effects from the depth direction (Horgue et al., 2013).

One effect is the viscous resistance from top and bottom substrates of the micromodel. Assuming trial velocity in the depth direction, Navier-Stokes equation can be integrated over the depth resulting an extra term:

$$\frac{\partial \rho \mathbf{u}}{\partial t} + \nabla \cdot (\rho \mathbf{u}\mathbf{u}) = -\nabla p + \nabla \cdot (2\mu \mathbf{E}) + \mathbf{f}_v - \frac{12\mu}{h^2}\mathbf{u} \tag{11}$$

where h is the depth of the micromodel.

The other effect is interface shape change due to the presence of top and bottom substrates. This effect can be geometrically approximated into an extra curvature term for smooth α:

$$k = -\nabla \cdot \left(\frac{\nabla \alpha}{\|\nabla \alpha\|}\right) - \frac{2}{h}\cos\theta \tag{12}$$

This corrected-two-dimensional model was implemented into interFoam solver of OpenFOAM.

3. Experiments simulated in this study

In this study we employ VOF method to simulate two-phase flow in domains of three different geometry complexities: a smooth glass tube and two micromodels of different designs.

3.1. Capillary rise experiment

This experiment was taken from Heshmati and Piri (2014), details can be found there. In the experiment a smooth glass tube of internal diameter 1 mm was vertically held with a Petri dish placed below it. To eliminate any curvature effects from edge of the dish, dish diameter was chosen as 9 cm. The glass tube was lowered slowly until it touched the water in the dish. The glass tube is water wet with zero static contact angle. Driven by capillary force, water will invade upwards into the tube. Water-air front was recorded during the process. Due to competition of capillary force, viscous force and gravity, imbibition front moves with decreasing speed and finally reaches at a steady position where capillary force balances with gravity.

3.2. Micromodel experiments

The micromodel experimental setup and hydrodynamic part of the experiment is shown in Fig. 1, details of the experimental system can be found at Karadimitriou et al. (2014). Two ends of the micromodel were connected with reservoirs where pump system controlled the pressure and pressure transducer measured the pressure. The image acquisition system can record the fluid distribution in the micromodel over time. Information like saturation, interfacial area can be obtained from image analysis of the micromodels. Micromodel was fabricated of Poly-Di-Methyl-Siloxane (PDMS). PDMS is hydrophobic, so flurinert was used as wetting phase and dyed water was used as non-wetting phase for better visualization. Drainage experiments were conducted with fixed boundary pressure drop. Initially the micromodel was filled with wetting phase flurinert with its inlet and outlet connected with non-wetting phase reservoir and wetting phase reservoir, respectively. Then, pressure in the non-wetting phase reservoir was increased and non-wetting phase invaded into micromodel as wetting phase receded into wetting phase reservoir. Flow distributions in the micromodels were recorded over time to be used in later numerical simulation comparison.

Two micromodels of different geometries and topologies were used in the experiments: (1) The first micromodel (hereafter referred to as micromodel 1) is shown in Fig. 2 with a random distribution of round pillars, and depth of the micromodel is 100 μm. In the dynamic drainage experiment, pressure difference between inlet and outlet was set as 1860 Pa. (2) The second micromodel (hereafter referred to as micromodel 2) is shown in Fig. 3 with depth of 40 μm, the size of the micro-model is 5 mm by 30 mm. The network topology was generated using Delaunay triangulation, which is considered to be a good approximation to a natural porous medium. With a total of 3000 pore bodies and nearly 9000 pore throats, geometry of micromodel 2 is bigger and more complex than micromodel 1. In the dynamic drainage experiment, pressure difference between inlet and outlet was set as 6300 Pa.

4. Simulation results and discussion

4.1. Verification of corrected-two-dimensional model

To test whether the corrected 2D model can adequately account for effects of the third dimension, it was compared to the full 3-dimensional model. The comparison was done for drainage in a

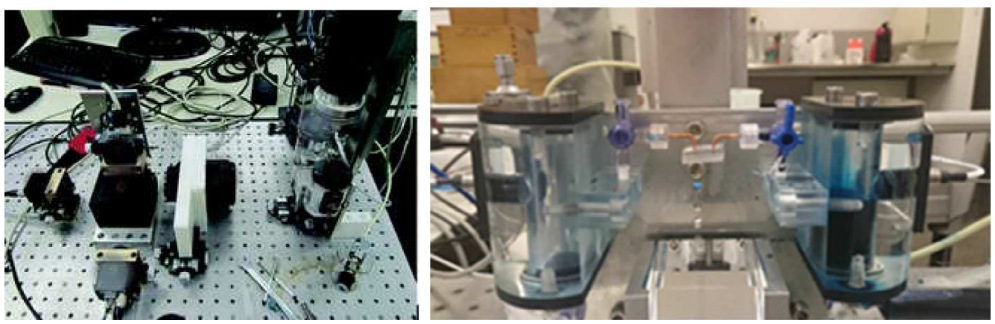

(a) Experimental setup (b) Hydrodynamic part of the experiment system

Fig. 1. Experimental setup and hydrodynamic part of the system.

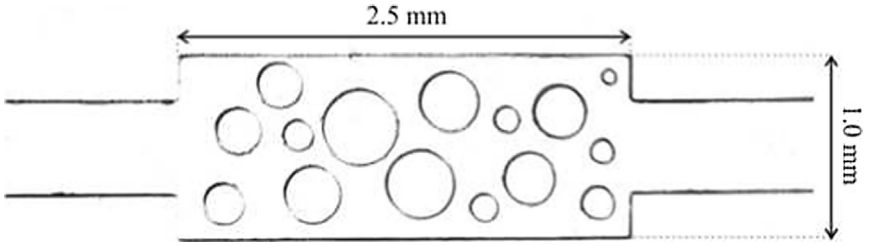

Fig. 2. Micromodel 1.

Fig. 3. Micromodel 2.

single duct with square cross section under pressure drop of 6000 Pa. The length of the conduct is 600 μm, with cross section of 40 μm × 40 μm. Half of the domain (600 μm× 40 μm × 20 μm) is simulated in 3D and mesh independence test for 3D simulations is shown in Fig. 4. Four sets of mesh size are tested: 300 × 20 × 10, 240 × 16 × 8, 150 × 10 × 5, and 120 × 8 × 4. Data from mesh size of 300 × 20 × 10 is compared with 2D simulation. Saturation of flurinert during drainage for 3D and corrected-2D simulation is shown in Fig. 5.

Snapshots of the interface position at $t = 0.004$ s are shown in Fig. 6. Interface in 2D simulation is one-dimensional, while in 3D it still poses two-dimensional shape, as can be seen in Fig. 7. Here we zoom into the interface region and only domain with $\alpha < 0.99$ is shown.

For this simple geometry, corrected 2D model can well recover the full 3D model. With complex pore geometry, assumption in Section 2.2 of interface shape and velocity field may fail, and corrected 2D model could introduce errors. However, to save computational time, corrected 2D model is employed for simulations of two micromodel experiments.

4.2. Capillary rise experiment

Fluid properties used in capillary rise simulation is shown in Table 1. Imbibition front position as a function of time from simulation and experiment is compared in Fig. 8. For this experiment of simple geometry, we observed good agreement between simulation and experimental data. This comparison shows fair validity of the VOF method in this case. This corresponds to the fact that validity of Washburn equation has been tested for capillary radius of several μm (Zhmud et al., 2000). One issue to mention: computational domain should include part of the dish where we impose hydrostatic pressure boundary condition and simulation with only capillary tube will result in faster invasion than experiment.

4.3. Micromodel experiments

Same fixed pressure drop boundary conditions were imposed in simulations as in experiments (See Section 3.2). Table 1 gives fluid properties used in simulation (Kunz et al., 2015). We are interested mainly in two aspects: (1) How is the flow pattern agreement between simulation and experiment? (2) Can we capture the dynamics of the invasion process?.

4.3.1. Primary drainage experiment in micromodel 1

Micromodel 1 has two long ducts as inlet and outlet. Right before the experiment, the initial interface position is out of the camera visualization domain. So, it is difficult to set the same initial condition as that in experiment. We tested simulations with

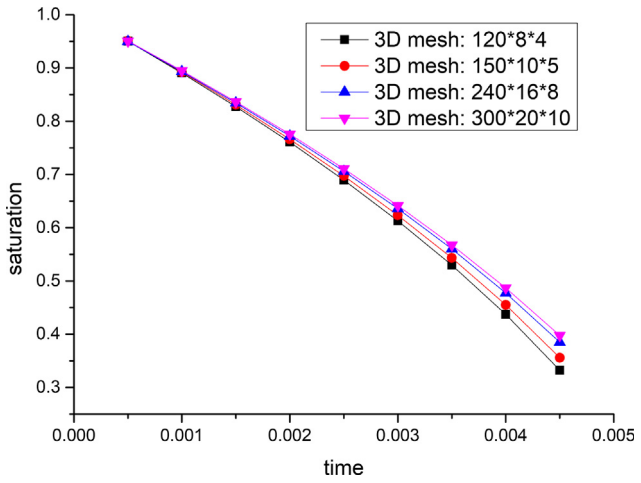

Fig. 4. Mesh independence test for drainage in 3D duct.

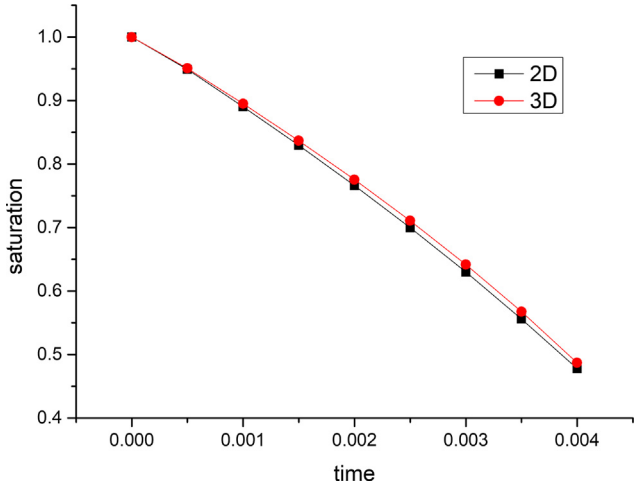

Fig. 5. Flurinert saturation during drainage in 2D and 3D duct.

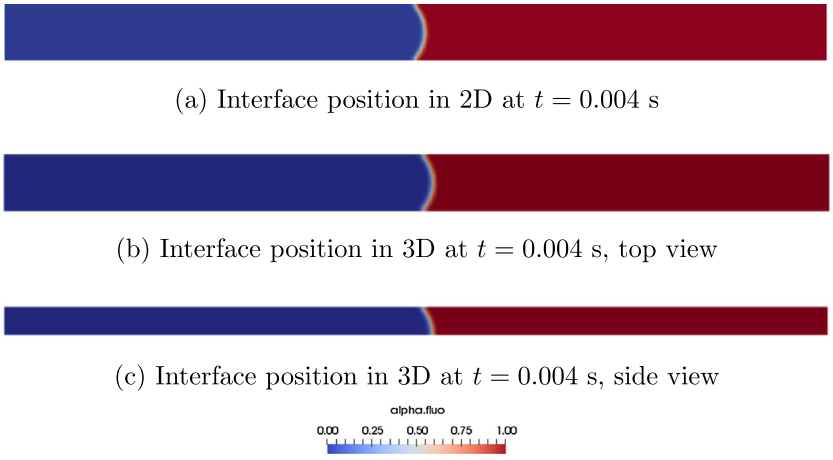

Fig. 6. Interface position at $t = 0.004$ s for 2D and 3D comparison.

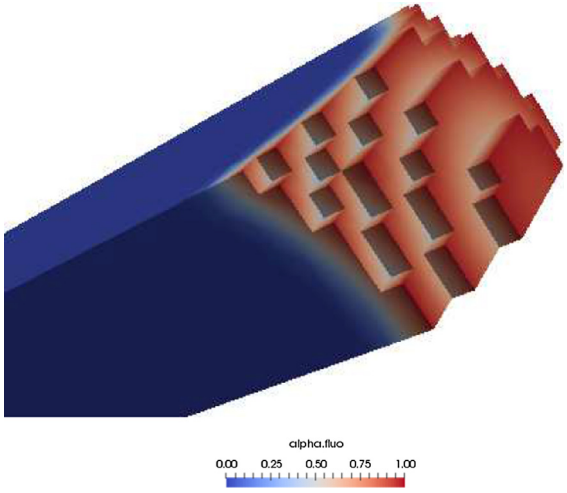

Fig. 7. Domain with $\alpha < 0.99$ around the interface in 3D.

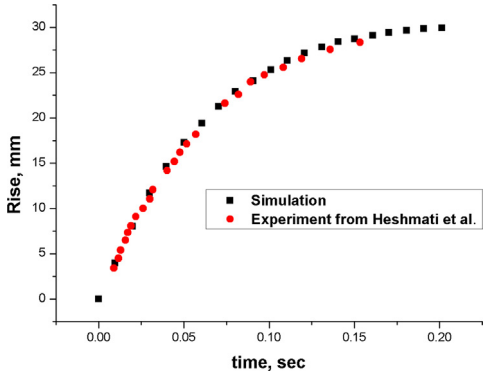

Fig. 8. Capillary rise comparison between experiment and simulation.

different initial interface positions, the results are quite close to each other. Here we select one of the simulations in comparison with experiment as shown in Fig. 9 and time zero is set based on close flow patterns between simulation and experiment. Although the initial conditions between simulation and experiment are different, for this relatively simple geometry, experimental flow patterns are well reproduced. In terms of kinetics we cannot reproduce experimental results satisfactorily. There are more energy dissipations and/or higher capillary barriers in experiments resulting in slower displacement.

4.3.2. Primary drainage experiment in micromodel 2

As shown in Fig. 10, simulation differs much more from experiment in terms of both dynamics and flow pattern. Invasion happened much slower in experiment than in simulation, which means that more resistance exists in experiments, the same as in micromodel 1. Furthermore, flow pattern was poorly predicted against experiment.

4.4. Discussions

Two-phase flow in three porous media of different geometry complexities are simulated, both flow pattern and process dynamics are compared with experiment.

For capillary rise experiment, the smooth glass tube, the regular geometry and the well correspondence of initial condition and boundary condition between simulation and experiment may help for satisfactorily reproducing the experimental measurement.

Disagreement in flow dynamics between simulation and experiment measurement may be attributed to possible pressure loss at connection between computational domain and pressure measurement points. Invisible roughness on the wall may also introduce

Table 1
Material properties used in simulations.

Specification	Symbol	Value		Unit
		Capillary	Micromodel	
Contact angle	θ	0	40	degree
Interfacial tension	σ^{wn}	0.072	0.058	kg s^{-2}
Wetting fluid viscosity	μ^{w}	0.001	0.047	kgm^{-1} s^{-1}
Non-wetting fluid viscosity	μ^{nw}	1.81×10^{-5}	0.001	kgm^{-1} s^{-1}

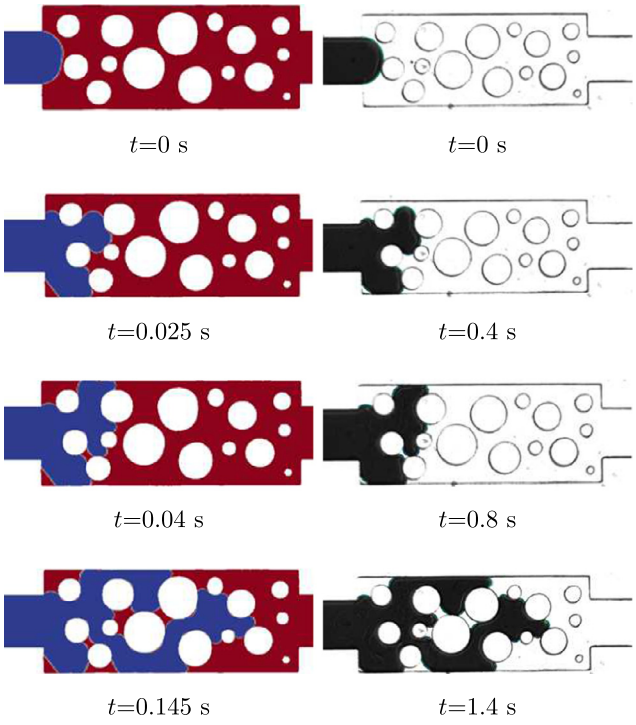

Fig. 9. Comparison between simulation and experiment for micromodel 1.

excess dissipation. Interface modeling, pinning of contact line and 3D effects, may introduce extra errors.

In VOF method, interface is not explicitly tracked and there exists a interface with several cells thickness. Volume fraction in this finite thickness layer is used to calculate the interface normal and curvature for the interface region, which could be inaccurate. Deshpande et al. (2012) reported a 10% error in interface curvature computation by VOF method from analytical value. In addition, interfacial tension is modelled as a volumetric force, at discrete level, we may have force imbalance between interfacial tension and other body forces. These two effects give rise to the so called "parasitic currents" (Wörner, 2012). This issue has been addressed by researchers using new interface reconstruction methods, such as piecewise linear interface construction method (PLIC) by Scardovelli and Zaleski (1999), parabolic reconstruction of surface tension (PROST) by Renardy and Renardy (2002) and contour-level surface force (CLSF) method by Shams et al. (2018). Spurious current is reported reduced effectively for fluid-fluid interface.

Invisible roughness may exist inside micromodel 1 and 2 due to fabrication. Pinning of contact line can play a role. A threshold stress value may exist below which there is no displacement of contact line. Excess force may be needed to move the contact line and keep it moving, especially for rough surface. de Gennes et al. (2004) discussed and determined the amount of energy needed to displace a contact line across a single roughness on an otherwise smooth surface: the fluid-fluid interface gets deformed until displacement happens and energy stored in the deformed interface is lost via viscous dissipation. These effects may not only give contact angle hysteresis but also introduce extra viscous losses near vicinity of interface and especially near the contact line where fluid may experience very high stress (Dullien, 1992; Kunz et al., 2018). In drainage experiment higher capillary pressure due to pinning will slow down the process. So it is rather probable that for same fixed pressure drop, in experiment more energy was consumed at the interface and contact line region than in numerical simulation. Numerical model produced faster invasion and this accumulate over time to give us the discrepancy in Figs. 9 and 10.

To save computational time, we have used 2D model. The corrected 2D model is derived with the assumption of trial depth-direction velocity and simplified interface geometry. For simple geometry, corrected 2D model can well recover the full 3D model. Modelling complex interface geometry, like merge/coalescence, is challenging physically and numerically even if 3D models are

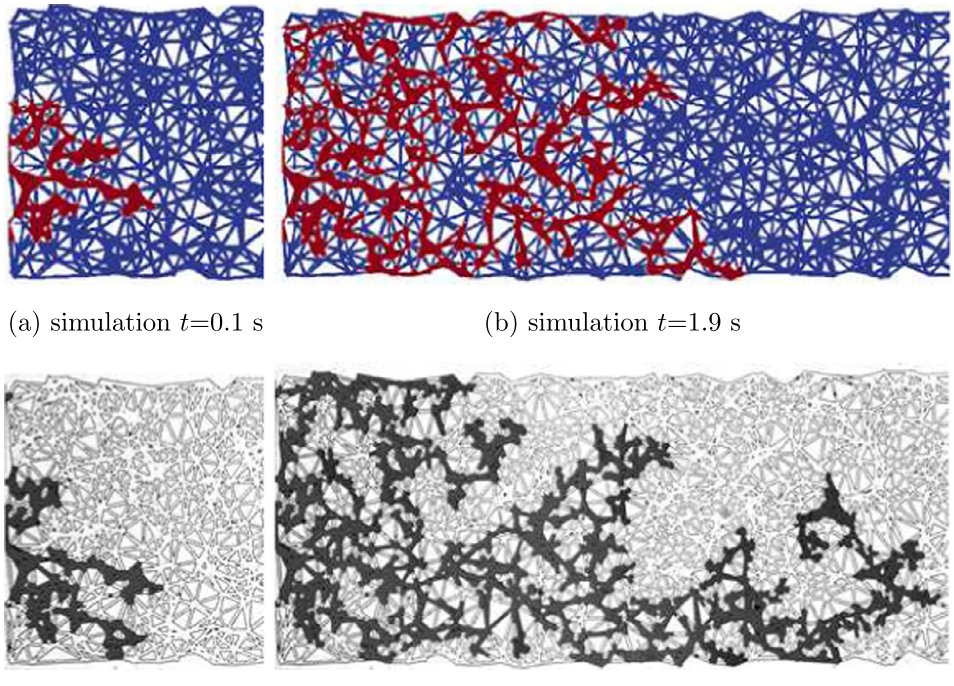

Fig. 10. Comparison between simulation and experiment for micromodel 2.

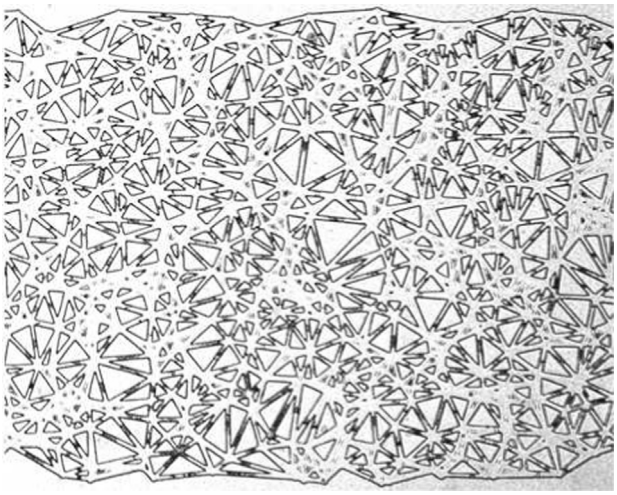

Fig. 11. Part of micromodel 2 showing roughness.

employed. In VOF method, interface shape change is not explicitly modelled, instead it comes from mass, momentum and volume fraction equations. In Fig. 9, the trapping of wetting phase at the left bottom corner at early time in the experiment is captured by the corrected 2D model. Later in the experiment, size of this trapped liquid bulb decreased through corner/film flow, and this is not captured by corrected 2D model. With corrected 2D model, we can simulate a relatively large domain and may lose some accuracy locally. The 3D effects of roughness inside the micromodel can give rise more errors (Ferrari et al., 2015).

In terms of flow pattern, for micromodel 1, good numerical results are probably due to stronger capillary effects than viscous effects and relatively simple geometry. For failure of flow pattern prediction of micromodel 2 in Fig. 10, this may be largely due to the small "islands"/roughness in the micromodel from fabrication process as shown in Fig. 11. On one hand, sizes of these "islands"/roughness are unknown; on the other hand, meshing around these "islands"/roughness would be an issue. So these "islands"/roughness were not included in our computational domain, and they may induce more viscous resistance and higher capillary barrier and thus also influence the flow pattern. Moreover, as discussed by Ling et al. (2017) and Fakhari et al. (2018), displacement in micromodel 2 could be sensitive to initial condition and boundary condition. Small discrepancy of initial condition and boundary condition between experiment and simulation may be amplified and lead to different flow pathways.

5. Summary and conclusion

Two-phase flow in three porous media of different geometry complexities are simulated, both flow pattern and process dynamics are compared with experiment. For simple geometry and smooth solid surface, like single capillary rise experiment, VOF simulation gave good agreement between simulation and experiment. For porous media with relatively simple geometry and possible rough surface, we may be able to predict the flow pattern while cannot capture the dynamics of the process like for micromodel 1. With increase of geometry complexity, we could fail in both flow pattern and dynamics prediction as in micromodel 2. Reasons for failure in reproducing experimental data are discussed: interface modeling, pinning of contact line, 3D effects and sensitivity of system to initial and boundary condition.

With the development of visualization techniques, high resolution images of pore structures can be obtained. Direct pore-scale simulations of multiphase flow using these data are appealing. However, modeling of interface and pinning of contact line in these detailed geometry are challenging. Furthermore, the system may be highly sensitive to boundary condition and initial condition and difficult to reproduce numerically. More work regarding benchmarking of pore-scale methods with better controlled experiments of different geometry complexities is needed (Yin, 2018). Also, how to practically make use of the high resolution structure data from visualization should be addressed. For capillary dominated situations, flow pattern is more controlled by porous media geometry. For simplicity, we could use quasi-static method (like medial axis method) to decide the flow pattern, and then calculate upscaled properties of interest by assuming appropriate boundary condition at liquid-liquid interface as done by Berg et al. (2016).

Acknowledgement

S.M. Hassanizadeh would like to thank European Research Council (ERC) for the support received under the ERC Advanced Grant Agreement No. 341225. Comments by anonymous reviewers, which led to the improvement of the article, are gratefully appreciated.

References

Berg, S., Rücker, M., Ott, H., Georgiadis, A., van der Linde, H., Enzmann, F., Kersten, M., Armstrong, R.T., de With, S., Becker, J., Wiegmann, A., 2016. Connected pathway relative permeability from pore-scale imaging of imbibition. Adv. Water Resour. 90, 24–35.

Blunt, M., 2001. Flow in porous media-pore-network models and multiphase flow. Curr. Opin. Colloid Interface Sci. 6 (3), 197–207.

Brackbill, J., Kothe, D., Zemach, C., 1992. A continuum method for modeling surface tension. J. Comput. Phys. 100 (2), 335–354.

Bultreys, T., De Boever, W., Cnudde, V., 2016. Imaging and image-based fluid transport modeling at the pore scale in geological materials: a practical introduction to the current state-of-the-art. Earth Sci. Rev. 155, 93–128.

de Gennes, P.G.D., Brochard-Wyart, F., Quéré, D., 2004. Capillarity and Wetting Phenomena. Springer.

Deshpande, S.S., Anumolu, L., Trujillo, M.F., 2012. Evaluating the performance of the two-phase flow solver interFoam. Comput. Sci. Discovery 5 (1), 014016.

Dullien, F.A.L., 1992. Porous Media: Fluid Transport and Pore Structure. Academic Press.

Fakhari, A., Li, Y., Bolster, D., Christensen, K.T., 2018. A phase-field lattice boltzmann model for simulating multiphase flows in porous media: application and comparison to experiments of CO_2 sequestration at pore scale. Adv. Water Resour. 114, 119–134.

Ferrari, A., Jimenez-Martinez, J., Borgne, T.L., Méheust, Y., Lunati, I., 2015. Challenges in modeling unstable two-phase flow experiments in porous micromodels. Water Resour. Res. 51 (3), 1381–1400.

Heshmati, M., Piri, M., 2014. Experimental investigation of dynamic contact angle and capillary rise in tubes with circular and noncircular cross sections. Langmuir: ACS J. Surf. Colloids 30 (47), 14151–14162.

Hirschler, M., Kunz, P., Huber, M., Hahn, F., Nieken, U., 2016. Open boundary conditions for isph and their application to micro-flow. J. Comput. Phys. 307, 614–633.

Horgue, P., Augier, F., Duru, P., Prat, M., Quintard, M., 2013. Experimental and numerical study of two-phase flows in arrays of cylinders. Chem. Eng. Sci. 102, 335–345.

Kaestner, A., Lehmann, E., Stampanoni, M., 2008. Imaging and image processing in porous media research. Adv. Water Resour. 31 (9), 1174–1187.

Kang, Q., Zhang, D., Chen, S., 2002. Unified lattice boltzmann method for flow in multiscale porous media. Phys. Rev. E 66 (5), 056307.

Karadimitriou, N.K., Hassanizadeh, S.M., Joekar-Niasar, V., Kleingeld, P.J., 2014. Micromodel study of two-phase flow under transient conditions: quantifying effects of specific interfacial area. Water Resour. Res. 50 (10), 8125–8140.

Kunz, P., Hassanizadeh, S., Nieken, U., 2018. A two-phase sph model for dynamic contact angles including fluid-solid interactions at the contact line. Transp. Porous Media 122 (2), 253–277.

Kunz, P., Zarikos, I.M., Karadimitriou, N.K., Huber, M., Nieken, U., Hassanizadeh, S.M., 2015. Study of multi-phase flow in porous media: comparison of SPH simulations with micro-model experiments. Transp. Porous Media 114, 581–600.

Ling, B., Bao, J., Oostrom, M., Battiato, I., Tartakovsky, A.M., 2017. Modeling variability in porescale multiphase flow experiments. Adv. Water Resour. 105, 29–38.

Oren, P.-E., Bakke, S., Arntzen, O., 1998. Extending predictive capabilities to network models. SPE J. 3 (December), 324–336.

Raeini, A.Q., Blunt, M.J., Bijeljic, B., 2012. Modelling two-phase flow in porous media at the pore scale using the volume-of-fluid method. J. Comput. Phys. 231 (17), 5653–5668.
Renardy, Y., Renardy, M., 2002. PROST: a parabolic reconstruction of surface tension for the volume-of-fluid method. J. Comput. Phys. 183 (2), 400–421.
Richards, L.A., 1931. Capillary conduction of liquids through porous mediums. Physics 1 (5), 318–333.
Scardovelli, R., Zaleski, S., 1999. Direct numerical simulation of free-surface and interfacial flow. Annu. Rev. Fluid Mech. 31, 567–603.
Shams, M., Raeini, A.Q., Blunt, M.J., Bijeljic, B., 2018. A numerical model of two-phase flow at the micro-scale using the volume-of-fluid method. J. Comput. Phys. 357, 159–182.
Van Genuchten, M.T., 1980. A closed-form equation for predicting the hydraulic conductivity of unsaturated soils. Soil Sci. Soc. Am. J. 44 (5), 892–898.
Weller, H.G., Tabor, G., Jasak, H., Fureby, C., 1998. A tensorial approach to computational continuum mechanics using object-oriented techniques. Comput. Phys. 12 (6), 620–631.
Wooding, R.A., Morel-Seytoux, H.J., 1976. Multiphase fluid flow through porous media. Annu. Rev. Fluid Mech. 8 (1), 233–274.
Wörner, M., 2012. Numerical modeling of multiphase flows in microfluidics and micro process engineering: a review of methods and applications. Microfluid. Nanofluid. 12 (6), 841–886.
Xu, Z., Liu, H., Valocchi, A.J., 2017. Lattice Boltzmann simulation of immiscible two-phase flow with capillary valve effect in porous media. Water Resour. Res. 53 (5), 3770–3790.
Yin, X., 2018. Pore-scale Mechanisms of Two-phase Flow in Porous Materials: Volume-of-Fluid Method and Pore-network Modelling (Ph.D thesis). Utrecht University.
Zhmud, B., Tiberg, F., Hallstensson, K., 2000. Dynamics of capillary rise. J. Colloid Interface Sci. 228 (2), 263–269.